Design of Donor Oligomers To Produce Parallel Spins upon Electron Transfer

H. Mizouchi, A. Ikawa, and H. Fukutome*

Contribution from the Department of Physics, Kyoto University, Kyoto 606, Japan

Received October 25, 1994[⊗]

Abstract: Donor oligomers that give parallel spins upon electron transfer (ET) are designed. Tetrathiafulvalenes (TTFs) or tetraselenafulvalenes (TSFs) are linked with bonds >C=Y (Y = CH_2, O, S, $C(CN)_2$) that yield dynamic spin polarization (DSP) in favor of parallel spins between cation radicals of adjacent donors. Donors in these oligomers are not linked by planar because of steric hindrance. Planar oligomers are designed by adding a −S− bridge in the linkage of two donors. Oligomers linked with a metaphenylene group are also examined. π electronic structures are calculated by the Pariser−Parr−Pople (PPP) model in the unrestricted Hartree−Fock (UHF) approximation using the Mataga−Nishimoto (M−N) or Ohno potential. Dications of all the dimers have the triplet UHF ground state. The DSPs, and consequently the singlet−triplet energy gaps (S−T gaps), are much larger in the M−N potential than the Ohno one. The S−T gaps are much larger in the planar dimers than in the nonplanar ones. Cation radicals of trimers and tetramers have quartet and quintet UHF ground states, respectively. Donor abilities and orbital energy gaps of oligomers and their cation radicals are studied.

1. Introduction

Much attention has been paid to synthesized organic ferromagnets. Some success in getting organic ferromagnetic crystals has been achieved. Some alternating stacks of donors and acceptors, in which donors contain transition metals, make ferromagnetic crystals.[1] The ferromagnetism was interpreted to arise from the McConnell mechanism[2] in which the triplet states in the donors with transition metals are essential. Some crystals of stable nitroxide radicals have been found to be ferromagnetic.[3] A simple rule for a crystal of nitroxide radicals to be ferromagnetic has been proposed.[3]

The oldest design of high-spin molecules was based on the following principle.[4] If radicals are distributed along a π-conjugated system, an alternating dynamic spin polarization (DSP)[5] is induced in the π system. If the phase of the DSP at all the radical sites is the same, the DSP stabilizes the state in which all the spins of the radical are parallel, namely, the highest-spin ground state is realized. *m*-Phenylene-linked polycarbenes have been synthesized, proving the correctness of this principle.[6] Di-, tri-, ..., and hexacarbenes have been shown to have the ground states with S = 2, 3, ..., and 6.

Though this principle is powerful, it is not easy to synthesize molecules to give very large spins. To overcome this difficulty, we have designed polaronic ferromagnetic polymers[7] in which polymers themselves have no radical spins but produce polarons upon doping and the adjacent polaron spins are parallelly coupled by the DSP produced by them. Some such polymers have been synthesized by Dougherty's group.[8−10] At low dopings, two kinds of such polymers have given parallel spin clusters of five and nine polarons on average, respectively. However, the fraction of magnetic domains has been small, and at high dopings, the average spin has decreased irreversively, to $^1/_2$, suggesting the occurrence of reactions between polarons.

High-spin molecules such as polycarbenes and polaronic ferromagnetic polymers also are difficult to crystallize. We have theoretically designed[11] donor oligomers which give the parallel spin ground state upon electron transfer (ET), owing to the DSP produced by their cation radicals. This idea is similar to the polaronic ferromagnetic polymers, but doping may be made by ET in solution and donor cations and anion counterions may crystallize. Therefore, we may expect production of new magnetic crystals. In this paper, we give a detailed theoretical account of the idea.

As our donor unit, we use tetrathiafulvalene (TTF) and tetraselenafulvalene (TSF). Donors are linked in the following three ways where X = S or Se and Y = CH_2, O, S, or $C(CN)_2$.

I)

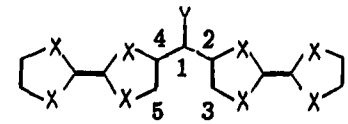

II)

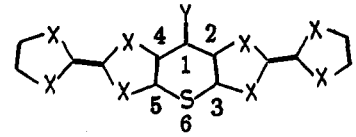

III)

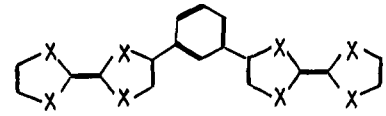

[⊗] Abstract published in *Advance ACS Abstracts*, February 15, 1995.

(1) Miller, J. S.; Epstein, A. J. *Angew. Chem., Int. Ed. Engl.* **1994**, *33*, 385−415.
(2) McConnell, H. M. *J. Chem. Phys.* **1963**, *39*, 1910.
(3) Awaga, K.; Sugano, T.; Kinoshita, M. *Chem. Phys. Lett.* **1991**, *190*, 349−352; **1992**, *195*, 21−24.
(4) Mataga, N. *Theor. Chim. Acta* **1968**, *10*, 372−376.
(5) Kollmar, H.; Staemmler, V. *J. Am. Chem. Soc.* **1977**, *99*, 3583−3587.
(6) Itoh, K. *Pure Appl. Chem.* **1978**, *50*, 1251−1259. Teki, Y.; Takui, T.; Itoh, K.; Iwamura, H.; Kobayashi, K. *J. Am. Chem. Soc.* **1983**, *105*, 3722−3723. Fujita, I.; Teki, Y.; Takui, T.; Kinoshita, T.; Itoh, K.; Miko, F.; Sawai, Y.; Iwamura, H.; Izuoka, A.; Sugawara, T. *J. Am. Chem. Soc.* **1990**, *112*, 4074−4075. Furukawa, K.; Matsumura, T.; Teki, Y.; Kinoshita, T.; Takui, T.; Itoh, K. *Mol. Cryst. Liq. Cryst.* **1993**, *232*, 251−260.
(7) Fukutome, H.; Takahashi, A.; Ozaki, M. *Chem. Phys. Lett.* **1987**, *133*, 34−38.

0002-7863/95/1517-3260$09.00/0

All these links give parallel spin unrestricted Hartree–Fock (UHF) ground states in the Pariser–Parr–Pople (PPP) approximation of these oligomers, as we shall see in this paper.

This paper is organized as follows. We discuss in section 2 the stable geometries of the dimers **I** and give the method of UHF calculations. We give in section 3 the singlet–triplet energy gaps (S–T gaps) and π electron and spin densities of the dications of the dimers. We show in section 4 orbital energy spectra and structures of some orbitals in the neutral and triplet dication states of the dimers. We consider in section 5 trimers and tetramers of these donors. We summarize in section 6 our results and give some discussions.

2. Geometries and Method of UHF Calculations

2.1 Geometries of the Dimers. To obtain the geometries of the dimers **I**, **II**, and **III** and those of the corresponding oligomers, we use the data of TTF,[12] and TSF,[13] and connecting bonds.[14–16] The dimers have three conformers. The donors in these conformers have steric

I) A and A′

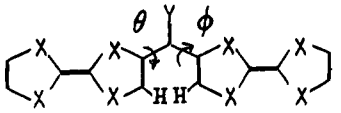

I) B and B′

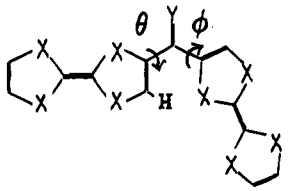

I) C and C′

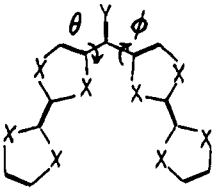

hindrances between the nearest neighboring atoms. The twisting angles θ and ϕ are determined so the distance between the nearest neighboring atoms is at the zero point of the Lennard-Jones potential between them.[16] In the conformers **A** and C, the twisting angles θ and ϕ are assumed to be equal, $\theta = \phi$, so that they have symmetric structures, but in **A′**, **C′**, **B**, and **B′**, the twisting is assumed to occur in only one of θ or ϕ.

Table 1. Bond Angles in Conformers of **I**

conformer	X	θ (deg)	ϕ (deg)
A	S	26.58	26.58
	Se	26.43	26.43
A′	S	0.00	51.54
	Se	0.00	51.28
B	S	0.00	69.25
	Se	0.00	69.77
B′	S	56.28	0.00
	Se	57.96	0.00
C	S	39.87	39.87
	Se	41.02	41.02
C′	S	0.00	72.06
	Se	0.00	74.83

Table 2. π Energies of the Triplet Ground States of Conformers of **I** with X = S and Y = CH_2

conformer	E_T (eV) M–N	E_T (eV) Ohno
A	−444.609	−451.807
A′	−444.433	−451.652
B	−444.159	−451.391
B′	−444.219	−451.410
C	−443.980	−451.156
C′	−443.942	−451.117

Table 3. Energy Gaps between the Singlet and Triplet Ground States of **I**, **II**, and **III**

X	Y	$E_S - E_T$ (meV) M–N	$E_S - E_T$ (meV) Ohno
		I	
S	CH_2	14.41	0.54
	O	12.38	0.21
	S	17.53	0.80
	$C(CN)_2$	16.71	0.78
Se	CH_2	11.17	0.19
	O	11.56	0.12
	S	15.84	0.38
	$C(CN)_2$	15.13	0.41
		II	
S	CH_2	57.26	5.43
	O	24.75	1.89
	S	47.76	4.99
	$C(CN)_2$	52.93	5.80
Se	CH_2	38.16	2.28
	O	15.29	1.57
	S	34.34	2.73
	$C(CN)_2$	22.31	1.19
		III	
S		7.42	0.21
Se		5.09	0.04

In symmetric conformers, the twistings around θ and ϕ are equivalent, but in asymmetric conformers, they are not so that **B** and **B′** have inequivalent structures. The values of the twisting angles θ and ϕ in these cases are listed in Table 1.

The geometries of **II** are assumed to be planar. In the connecting ring part, the bond lengths are fixed to the observed values C_1–C_2 = 1.446 Å, C_2–C_3 = 1.314 Å, and C_3–S_6 = 1.745 Å that are the average of the C–S distances in TTF. The angles θ_1, θ_2, and θ_3 are optimized so as to minimize $\sum_i(\theta_i - \bar{\theta}_i)^2$, where the $\bar{\theta}_i$ values, i = 1, 2, or 3, are observed bond angles in typical molecules, under the constraint that the atoms make a ring with the bond lengths given above and the bending force constants of C_1, C_2, and C_3 are the same. The angles obtained are θ_1 = 119.6°, θ_2 = 122.1°, and θ_3 = 130.3°. The bond angle of the connecting S becomes θ_6 = 95.7° which is close to the bond angle 94.4° of S's in TTF. Therefore, the planar ring connection in **II** is not unnatural except for a little large θ_3. We consider only trans geometries of **III** which are assumed to be planar, though there may be some twisting in the *m*-phenylene connection.

(8) Dougherty, D. A.; Kaisaki, D. A. *Mol. Cryst. Liq. Cryst.* **1990**, *183*, 71–79.
(9) Kaisaki, K. A.; Chang, W.; Dougherty, D. A. *J. Am. Chem. Soc.* **1991**, *113*, 2764–2766.
(10) Dougherty, D. A.; Jacobs, S. J.; Silverman, S. K.; Murray, M. M.; Shultz, D. A.; West, A. P.; Clites, J. A. *Mol. Cryst. Liq. Cryst.* **1993**, *232*, 289–304.
(11) Mizouchi, H.; Ikawa, A.; Fukutome, H. *Mol. Cryst. Liq. Cryst.* **1993**, *233*, 127–132.
(12) Blessing, R. H.; Coppens, P. *Solid State Commun.* **1974**, *15*, 215–221.
(13) Bechgard, K.; Kitenmacher, T. J.; Bloch, A. N.; Cowan, D. O. *Acta Crystallogr.* **1977**, *B33*, 417–422.
(14) Geiser, U.; Wang, H. H.; Schlueter, J. A.; Hallenbeck, S. L.; Allen, T. J.; Chen, M. Y.; Kao, H.-C. I.; Carlson, K. D.; Gerdom, L. E.; Williams, J. M. *Acta Crystallogr.* **1988**, *C44*, 1544–1547.
(15) Bencharif, P. M.; Ouahab, L. *Acta Crystallogr.* **1988**, *C44*, 1514–1516.
(16) *Chemistry Handbook*, 3rd ed.; Chemical Society of Japan: Maruzen, Tokyo, 1984; Vol. II, pp 649–722.

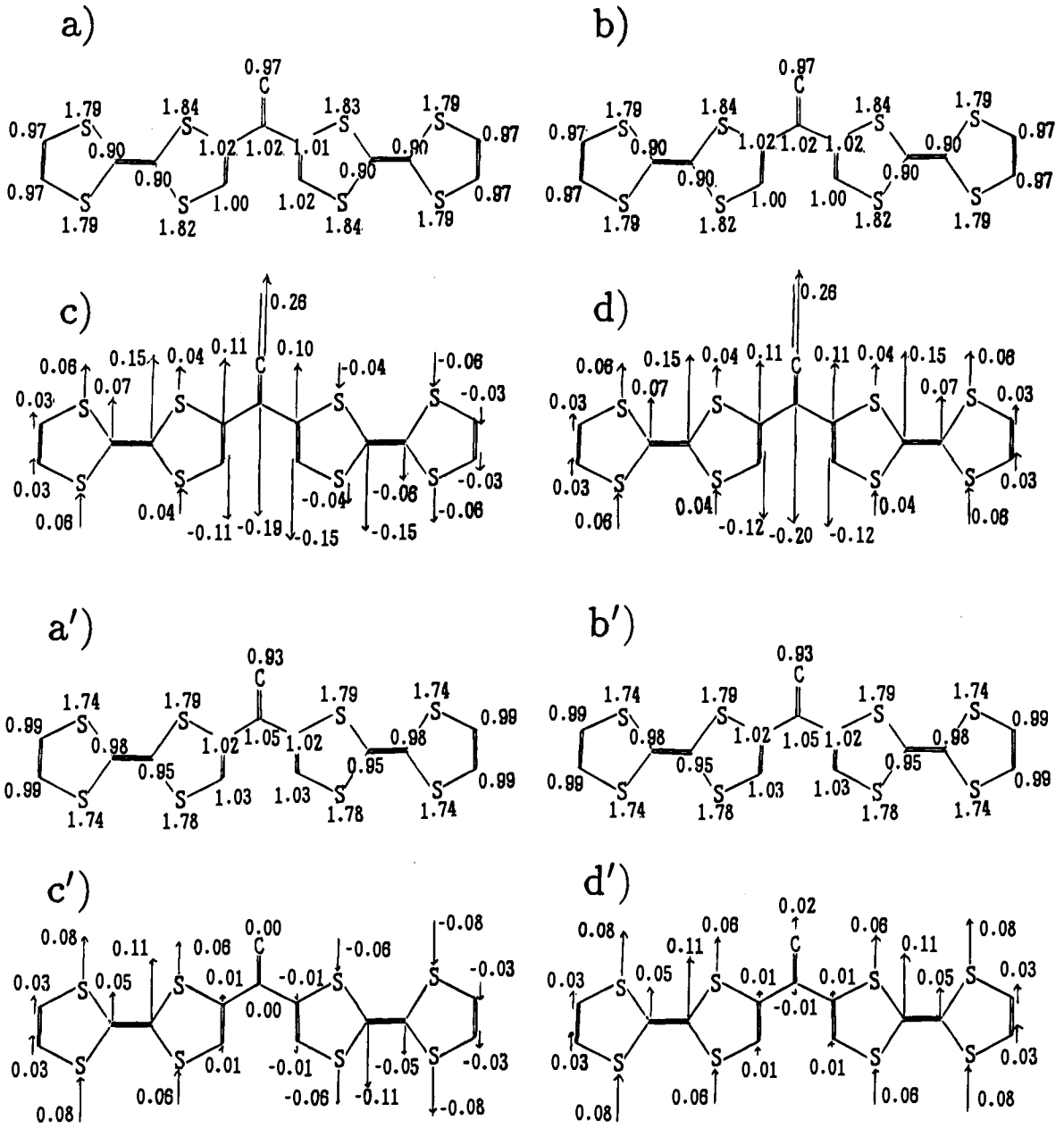

Figure 1. π electron density (ED), a and b, and spin density (SD), c and d, structures of **I** with X = S and Y = CH_2 in the M−N potential case. The cases a and c show the EDs in the singlet and triplet dication states, respectively, and b and d show the SDs in those states. The cases a′, b′, c′, and d′ show the corresponding quantities in the Ohno potential case.

2.2 Method of UHF Calculations. We have to calculate electronic structures of oligomers of types **I**, **II**, and **III**. Because of the large dimensions, we are forced to use a semiempirical model. We first need to check reliabilities of semiempirical models.[17] Since we have to calculate spin structures of radicals, models neglecting the electron−electron Coulomb interaction, such as the extended Hückel (EH) model, cannot be used because the DSP effects with which we are now mainly concerned arise from the electron−electron Coulomb interaction.

There was an ab initio MO calculation of TTF.[18] It showed that all the orbitals from the highest occupied molecular orbital (HOMO) to the fourth HOMO were of type π. The PPP model[19] gave the orbitals of the same symmetries and a similar orbital energy spectrum up to the fourth HOMO. The EH model[20] gave similar orbitals. A polarized UPS experiment[20] supports this assignment. The full valence electron semiempirical models, however, gave results in disagreement with the ab initio result. The CNDO/S calculation for TTF[21] gave the correct HOMO of b_{1u} π symmetry but the second HOMO of b_{1g} σ symmetry in disagreement with the ab initio result of b_{3g} π. We have made an INDO calculation for TTF. It, however, gave an incorrect result similar to the CNDO/S one with the HOMO (b_{1u} π), second HOMO (b_{3g} π), and third HOMO (b_{1g} σ). In evaluation of the energy of a twisted molecule, use of a full valence electron model is desirable. However, because of the unreliabilities of the CNDO and INDO models in TTF, we decided to use the PPP model though it may not be reliable in evaluation of the energies of twisted molecules.

The Hamiltonian of π electrons in the PPP model[17] is given by

$$H = \sum_{\mu,\nu,\sigma}\beta_{\mu\nu}\alpha^{\dagger}_{\mu\sigma}\alpha_{\nu\sigma} + \sum_{\mu,\sigma}\gamma_{\mu\mu}\eta_{\mu\sigma}\eta_{\mu-\sigma} + {}^1/_2\sum_{\mu,\nu}\gamma_{\mu\nu}\eta_{\mu}\eta_{\nu} + \sum_{\mu}U_{\mu\mu}\eta_{\mu} - \sum_{\mu,\nu}Z_{\mu}\gamma_{\mu\nu}\eta_{\nu} \quad (1)$$

where $\alpha_{\mu\sigma}$ and $\alpha^{\dagger}_{\mu\sigma}$ are the annihilation and creation operators at the

(17) Murrell, J. S.; Harget, A. J. *Semi-empirical self-consistent-field molecular orbital theory of molecules*; John Wiley & Sons Ltd.: London, 1972; pp 1−169.
(18) Tric, M.; Laidlaw, W. G. *Int. J. Quantum Chem.* **1982**, *11*, 557−563.
(19) Zahradnik, R.; Carsky, P.; Hünig, S.; Klesslich, G.; Schewtzov, D. *Int. J. Sulfur Chem.* **1971**, *C6*, 109−122.

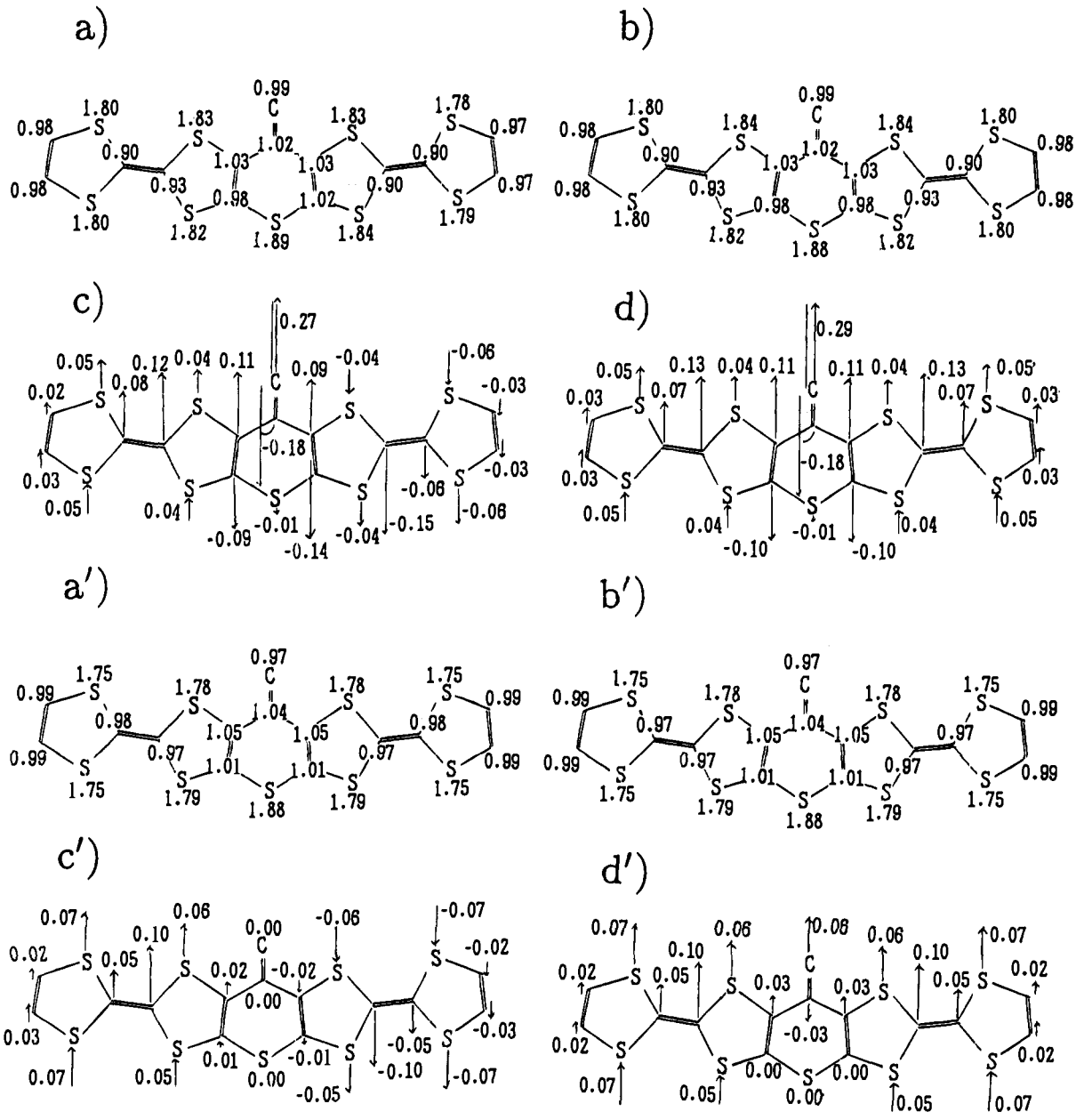

Figure 2. π EDs and SDs of **II** with X = S and Y = CH_2 in the M−N potential case where the cases a, b, c, and d are the same as in Figure 1. The cases a', b', c', and d' show the corresponding quantities in the Ohno potential case.

μth site, respectively, with spin $\sigma = \pm 1/2$, $\eta_{\mu\sigma} = \alpha^{\dagger}_{\mu\sigma}\alpha_{\mu\sigma}$ is the number operator of π electrons, and $\eta_\mu = \sum_\sigma \eta_{\mu\sigma}$. $\sum'_{\mu,\nu}$ is the sum over all μ and ν under the restriction $\mu \neq \nu$. The first term of eq 1 represents transfer interaction. The transfer integrals $\beta_{\mu\nu}$ are considered between only nearest neighbor sites μ and ν and are calculated in the Wolfsberg−Helmholz approximation[22]

$$\beta_{\mu\nu} = -k(I_\mu + I_\nu)S_{\mu\nu} \tag{2}$$

where I_μ is the ionization potential of the μth atom, $S_{\mu\nu}$ is the overlap integral between μ and ν and is calculated according to Mulliken et al.,[23] and the coefficient k (= 0.462) is determined by the averaged value of ethylene and benzene. In a bond twisting by an angle θ, $\beta_{\mu\nu}$ is reduced by cos θ.

The second and third terms of eq 1 represent on-site and different-site electron repulsions, respectively. The electron repulsion integrals $\gamma_{\mu\nu}$ are calculated both in the Mataga−Nishimoto (M−N)[24] and Ohno formulas.[25]

The fourth and fifth terms of eq 1 represent on-site and different-site core Coulomb attractions, respectively. If the atom of the μth site has one or two π electrons, $U_{\mu\mu} = -I_\mu$ or $U_{\mu\mu} = -(2I_\mu - A_\mu)$, respectively, where I_μ and A_μ are the ionization potential and the electron affinity of the μth site.[26] Z_μ is the valence number of the core of the μth site.

We use the UHF program with a direct optimization algorithm that is able to calculate instabilities.[27] The convergence condition is that the differences of the density matrices in consecutive iterations become smaller than 10^{-4}. If the instability matrices have negative eigenvalues, we calculate the solution with the lowest energy. The UHF ground state has no instability.

(20) Gleiter, R.; Schmidt, E.; Cowan, D. O.; Ferraris, J. P. *J. Electron Spectrosc. Relat. Phenom.* **1973**, *2*, 207−210.
(21) Ladik, J.; Karpfen, A.; Stollhoff, G.; Fulde, P. *Chem. Phys.* **1975**, *7*, 267−277.
(22) Wolfsberg, M.; Helmholz, L. *J. Chem. Phys.* **1952**, *20*, 837−843.
(23) Mulliken, R. S.; Rieke, C. A.; Orloff, D.; Orloff, H. *J. Chem. Phys.* **1949**, *17*, 1248−1267.
(24) Mataga, N.; Nishimoto, K. *Z. Phys. Chem.* **1957**, *13*, 124−141.
(25) Ohno, K. *Theor. Chim. Acta* **1964**, *2*, 219−227.
(26) Hinze, J.; Jaffe, H. H. *J. Am. Chem. Soc.* **1962**, *84*, 540−546.
(27) Igawa, A.; Fukutome, H. *Prog. Theor. Phys.* **1975**, *54*, 1266−1281.

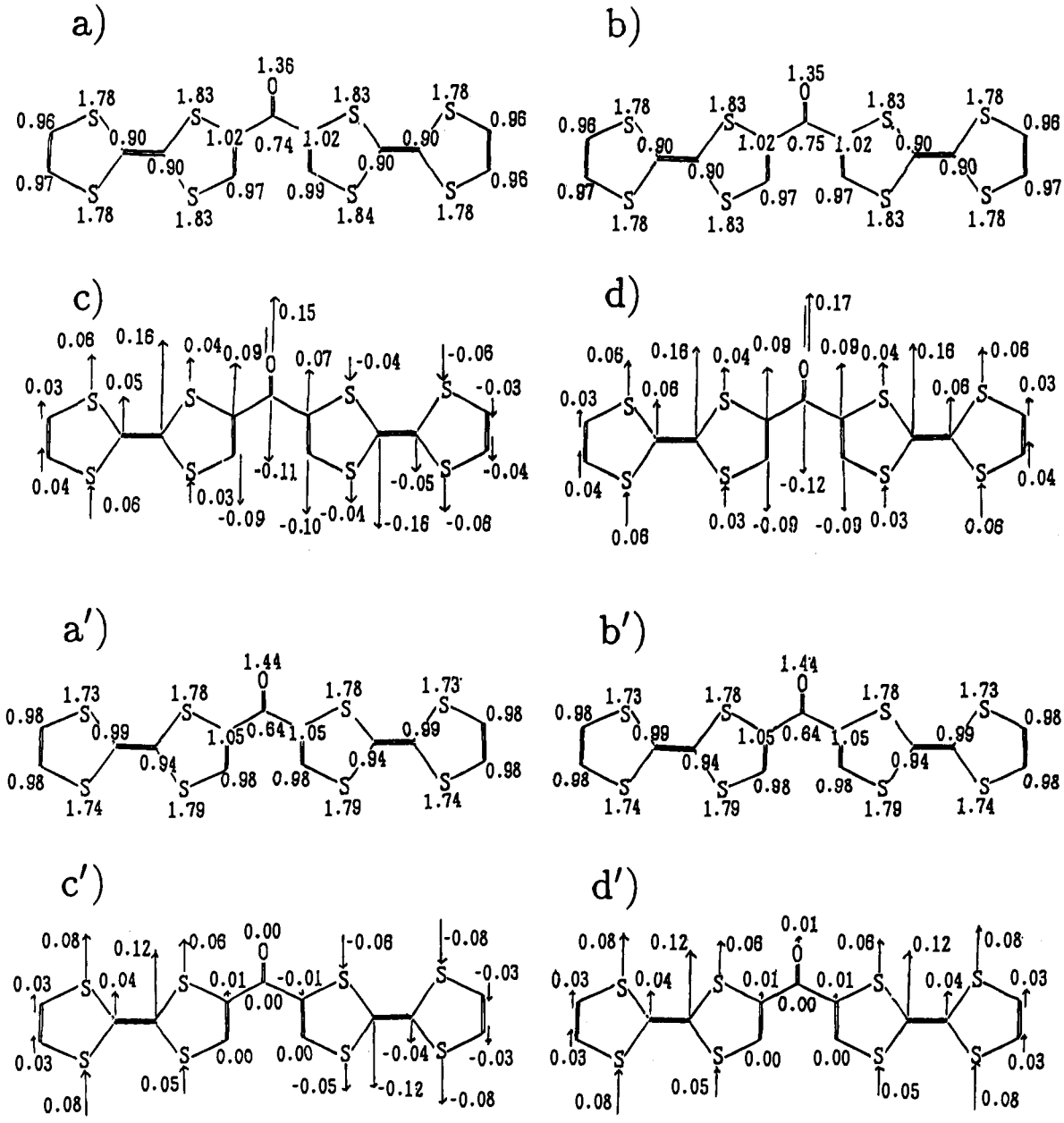

Figure 3. π EDs and SDs of **I** with X = S and Y = O. The cases a, b, c, and d and a', b', c', and d' are the same as in Figures 1 and 2.

The orbitals and their energies of the TTF monomer calculated by this model give the correct symmetries of the HOMO and second HOMO, and its orbital energy spectrum is in agreement with the experimental and the ab initio spectra up to the fourth HOMO.

3. Dication States

3.1 π Energies of Conformers of I. In the dications of all six conformers of **I**, the triplet ground states are more stable than the singlet ones. The π energies of the triplet dications of all the conformers of **I** with X = S and Y = CH_2 are listed in Table 2. This energy is the sum of the energies of the π electrons and the core−core repulsions. Table 2 shows that conformer **A** has the lowest π energy in both the M−N and Ohno potentials. In the dications of the other species of **I**, the conformer **A** is also the most stable in both the potentials. **A** has the smallest twisting angle, so this is the most stabilized by delocalization of π electrons. In addition, due to the geometry, **A** has the smallest core−core Coulomb repulsion. This is why **A** is the most stable conformer.

In the following sections, we show only the results of the molecules of **I** in the conformer **A**.

3.2 The S−T Gaps and π Electron Density and Spin Density Structures of I, II, and III. The S−T gaps of **I** in the conformer **A** and **II** and **III** in the dications are listed in Table 3.

All molecules have the triplet ground states in the dications and give much larger S−T gaps in the M−N potential than in the Ohno one. All the conformers of **II** give much larger S−T gaps than **I** in both the potentials, so planarity of molecules is considered as the reason for larger S−T gaps. This planarity increases the S−T gaps in the Ohno potential more than in the M−N one. In the case of Y = O, the S−T gaps are smaller than the other cases. The S−T gaps in the Ohno case of **I** are so small that inclusion of σ electrons and correlation beyond UHF may alter the order of the singlet and triplet states. All the conformers of **III** give very small S−T gaps.

π electron density (ED) and spin density (SD) of **I** and **II** with X = S and Y = CH_2 are shown in Figure 1 and Figure 2.

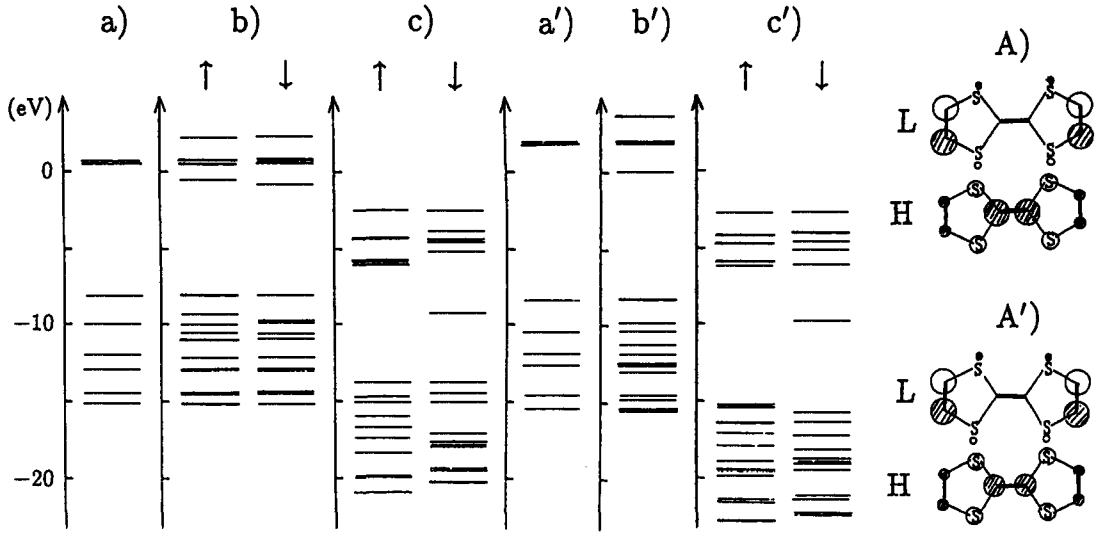

Figure 4. Orbital energy levels of TTF monomer (a), those of the dimer **I** with X = S and Y = CH_2 in the neutral (b) and triplet dication states (c) in the M−N potential case. The corresponding orbital energy levels in the Ohno potential case are shown in a′, b′, and c′. The structures of the LUMO (L) and HOMO (H) of TTF monomer in the neutral state in the M−N (A) and Ohno (A′) potential cases are also indicated. The signs and magnitudes of π MO's are indicated by unhatched (positive) and hatched (negative) circles with corresponding sizes.

The common points in the ED and SD of **I** and **II** are as follows.

(1) Spin delocalization appears on both TTFs (TSFs). When **I** and **II** become dications, holes are created mainly from the lone pairs of sulfur on TTF or selene on TSF, and both **I** and **II** are stabilized by delocalization of these holes. This is the origin of the spin delocalization. The hole delocalization is larger in the M−N case than in the Ohno case and as large in the triplet states as in the singlet states in both the M−N and Ohno cases.

(2) On the linking bonds, DSP appears except in the singlet states in the Ohno case where little DSP appears. The DSP is much smaller in the triplet states in the Ohno case than in both the singlet and the triplet states in the M−N case. In the M−N case, the large DSP not only appears on linking bonds but also extends to carbons adjacent to the linking bonds. In the case of Y = O, the DSP is much smaller than in the other cases, and especially in the triplet state in the Ohno case, the SD almost disappears on the carbons connected with the two TTFs (TSFs), as seen in Figure 3.

(3) Charge polarization (CP) on the linking bonds is always present. The CP is larger in the Ohno case than in the M−N case. It is large especially in the case of Y = O (Figure 3). In both the M−N and Ohno cases, the CP is as large in the triplet states as in the singlet states.

(4) The differences between X = S and Se are as follows. Hole delocalization on TSF is smaller than on TTF because the C−Se bond on TSF is long and the transfer integral is small.

The differences between the M−N and Ohno cases can be explained as follows. Let the on-site and nearest neighbor-site electron repulsion be γ_0 and γ_1, respectively. The relation between γ_0 and γ_1 is

$$\gamma_1 < \gamma_0/2 \qquad \text{(M−N)}$$

$$\gamma_1 > \gamma_0/2 \qquad \text{(Ohno)}$$

For example, in the case of a C−C bond with a bond length of 1.446 Å, γ_0 is the common value 11.13 eV and γ_1 is 5.256 eV in the M−N case and 7.433 eV in the Ohno case. As CP increases with γ_1 and the DSP with $\gamma_0 - \gamma_1$, the Ohno and M−N potentials give large CP and DSP, respectively.

The stability of the triplet states to the singlet states can be explained as follows. In the Ohno case, the stabilization seems to be due to DSP. It appears on the connecting bonds in the triplet states, though its amplitude is small (Figures 1d′ and 2d′), but it little appears in the singlet states (Figures 1c′ and 2c′). In the M−N case, the DSP appears both in the singlet and triplet states to a similar extent but with a little larger amplitude in the triplet states (Figures 1c and 2c). In the triplet states, the DSP on the linking bonds is not contradicting with the directions of spins of delocalized holes on the two TTFs (TSFs) (Figures 1d and 2d). In the singlet states, the spins of the holes in the two TTFs (TSFs) are opposite so that one of them contradicts with the DSP in the connecting bonds as seen in the right side TTF in Figures 1c and 2c. This may be the reason to increase the energies of the singlet states.

The ED and SD of **I** and **II** have the following differences.

(1) The DSP on the linking bonds of **II** is a little smaller than that of **I** in both singlet and triplet states in the M−N case. But in the triplet states in the Ohno case, the DSP of **II** is larger.

(2) On the connecting sulfur in **II**, the SD is very small in the M−N case and almost disappears in the Ohno case.

(3) The CP on the linking bonds of **II** is larger than that of **I** in both the M−N and Ohno cases.

The ED and SD of **III** is as follows. Holes on TTFs and TSFs have distributions similar to those in **I** and **II**. The DSP on atoms in linking bonds and adjacent carbons in donors are about one-half smaller than those in **I** and **II** in the M−N case. In the singlet state of the Ohno case, it is almost vanishing and very small in the triplet state, too. This small DSP makes the S−T gaps in **III** much smaller than those in **I** and **II**.

4. Structures of Some Orbitals, Donor Abilities, and Optical Gaps

4.1 Structures of Some Orbitals. In Figure 4, the orbital energy levels of TTF monomer, neutral and triplet dication states of **I** with X = S and Y = CH_2 in both the M−N and Ohno cases are given. The lowest unoccupied molecular orbital (LUMO) and HOMO of TTF monomer in the neutral states are also shown in Figure 4. The LUMO, HOMO, and second HOMO of **I** in the neutral and triplet dication states are given in Figure 5.

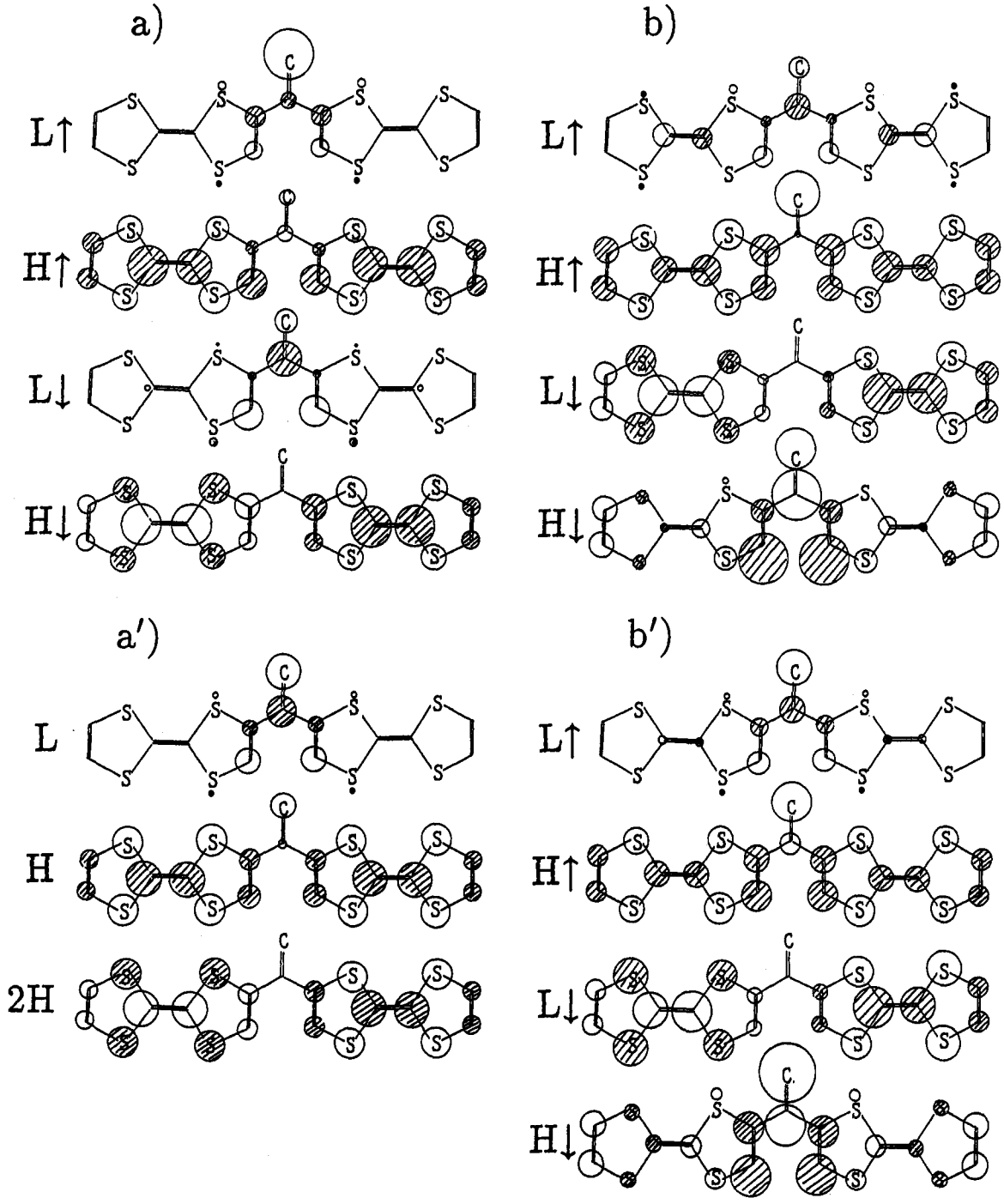

Figure 5. Structures of the LUMO (L), HOMO (H), and second HOMO (2H) of **I** with X = S and Y = CH_2 in the neutral state (a) and the triplet dication state (b) in the M−N potential case. The corresponding MO's in the Ohno potential case are shown in a′ and b′. The MO's with up and down spins are indicated by the corresponding arrows. The MO's without arrows show closed shells. Notations in MO's are the same as in Figure 4.

The characters of monomers of **I** and **II** in the neutral states are as follows. Both the HOMO and LUMO of monomers have little differences in structure between the Ohno and M−N cases (Figure 4, A and A′). In the M−N case, all of **I** and **II** are singlet diradicals even in the neutral states, while in the Ohno case, they are closed-shell molecules. In the Ohno case, the orbital energies of the HOMO and second HOMO are very close. They are symmetrical and antisymmetrical superpositions of the HOMO's of the two monomers (Figure 5a′). The LUMO's are symmetrical and have large MO coefficients on the linking bonds. The LUMO of the monomer is of nonbonding type as seen in Figure 4. Its half-fragments are contained in the second, third, and fourth LUMO's, which are of nonbonding type and nearly degenerate to the monomer LUMO. Therefore, the LUMO−HOMO gaps (L−H gaps) of the dimers are smaller than those of the monomers (Figure 4b′). When HOMO's or second HOMO's of **II** are symmetrical, C_3-S_6 and C_5-S_6 bonds are antibonding. In the M−N case, the up and down spin HOMO's correspond to the HOMO and second HOMO in the Ohno case. The up and down spin LUMO's have MO coefficients concentrated on the connecting bonds, but their MO coefficients have somewhat different distributions. The L−H gap also becomes smaller than the monomer (Figure 4b).

The characters of **I** and **II** in the triplet dications are as follows. If two electrons with down spins are eliminated, the

Table 4. Energies of the HOMO and the LUMO−HOMO Gaps in Monomers and the Differences of the Energies between the HOMO's of Monomer and Dimer and the LUMO−HOMO Gaps in Neutral Dimers **I** and **II**

	HOMO		LUMO−HOMO	
X	M−N	Ohno	M−N	Ohno
S	−8.096	−8.536	8.731	10.321
Se	−7.231	−7.395	7.781	9.089

		ΔHOMO[a]		LUMO−HOMO	
X	Y	M−N[b]	Ohno	M−N[b]	Ohno
		I			
S	CH_2	(↑)−0.034	−0.070	7.573	8.366
		(↓)−0.015		7.231	
	O	0.089	0.138	6.429	7.931
		0.055		6.478	
	S	0.076	0.155	6.488	7.347
		0.086		5.976	
	$C(CN)_2$	0.073	0.152	6.409	7.035
		0.067		5.820	
Se	CH_2	−0.019	−0.042	6.793	7.302
		−0.032		6.457	
	O	0.040	0.069	5.606	6.824
		0.002		5.715	
	S	0.068	0.103	5.181	6.271
		0.035		5.723	
	$C(CN)_2$	0.032	0.117	5.626	5.956
		0.058		5.018	
		II			
S	CH_2	(↑)−0.042	−0.311	7.543	8.393
		(↓)−0.365		7.477	
	O	0.029	0.075	6.656	8.197
		0.005		6.601	
	S	−0.112	0.051	6.020	7.567
		0.063		6.635	
	$C(CN)_2$	0.055	0.026	6.610	7.186
		−0.186		5.737	
Se	CH_2	−0.055	−0.130	6.781	7.481
		−0.169		6.858	
	O	−0.026	0.025	5.861	7.100
		−0.021		5.789	
	S	0.020	0.070	5.864	6.554
		−0.027		5.312	
	$C(CN)_2$	−0.064	0.004	5.257	6.467
		−0.010		5.691	

[a] ΔHOMO = HOMO(monomer) − HOMO(dimer). [b] In the M−N case, the up and down spin values are indicated in the upper and lower rows. All energies are in electronvolts.

LUMO (↓) has the same character as the second HOMO in the neutral state. The HOMO (↓) has the character of the third HOMO in the neutral state. It has large MO coefficients on the linking bonds (Figure 5, b and b′) and will contribute much to the DSP in triplet dications. The HOMO (↑) and LUMO (↑) retain characters similar to those in the neutral state, though the former has increased MO coefficients on the connecting bonds.

4.2 Donor Abilities and Optical Gaps. The differences of orbital energies of HOMO's between neutral monomers and neutral dimers and L−H gaps of neutral dimers are listed in Table 4.

This indicates that the donor abilities of **I** are less than the one of the corresponding monomer except in the case of Y = CH_2, and those of **II** are increased except in the case of X = S and Y = O in the M−N case and decreased except in the case of Y = CH_2 in the Ohno case. The L−H gaps determine the optical gaps. They have decreased values in all dimers in the order Y = CH_2 > O > S > $C(CN)_2$.

The L−H gaps of the doublet monocations of monomers and the triplet dications of dimers **I** and **II** are listed in Table 5.

Table 5. LUMO−HOMO Gaps (eV) in Doublet Monocations of Monomers and Triplet Dications of Dimers **I** and **II**

	LUMO−HOMO	
X	M−N	Ohno
S	(↑)7.863	9.468
	(↓)5.085	6.519
Se	7.422	8.619
	4.947	6.308

		I LUMO−HOMO		II LUMO−HOMO	
X	Y	M−N	Ohno	M−N	Ohno
S	CH_2	(↑)7.739	9.044	7.651	8.669
		(↓)4.526	5.955	3.610	5.031
	O	7.325	8.767	7.493	8.880
		5.097	6.652	4.440	6.141
	S	7.404	8.253	7.464	8.170
		4.726	6.191	3.855	5.412
	$C(CN)_2$	7.323	8.046	7.230	7.805
		4.547	5.917	3.672	5.133
Se	CH_2	6.805	7.663	6.975	7.725
		4.694	6.114	4.041	5.582
	O	6.151	7.163	6.354	7.403
		5.021	6.370	4.681	6.116
	S	6.288	6.757	6.438	6.974
		4.829	6.263	4.249	5.888
	$C(CN)_2$	6.248	6.608	6.350	7.098
		4.738	6.160	4.267	5.916

Table 6. Energy Gaps between Different Spin States in *N*-mers of **II** with Trans Connections and X = S and Y = CH_2

		gap (meV)	
N	spin state[a]	M−N	Ohno
2	$E(\uparrow\downarrow)-E(\uparrow\uparrow)$	57.26	5.43
3	$E(\uparrow\uparrow\downarrow)-E(\uparrow\uparrow\uparrow)$	40.61	6.00
	$E(\uparrow\downarrow\uparrow)-E(\uparrow\uparrow\uparrow)$	85.76	12.03
4	$E(\uparrow\uparrow\uparrow\downarrow)-E(\uparrow\uparrow\uparrow\uparrow)$	27.12	6.24
	$E(\uparrow\uparrow\downarrow\uparrow)-E(\uparrow\uparrow\uparrow\uparrow)$	59.32	12.38
	$E(\uparrow\uparrow\downarrow\downarrow)-E(\uparrow\uparrow\uparrow\uparrow)$	41.79	6.12
	$E(\uparrow\downarrow\uparrow\downarrow)-E(\uparrow\uparrow\uparrow\uparrow)$	58.15	12.49
	$E(\uparrow\downarrow\uparrow\downarrow)-E(\uparrow\uparrow\uparrow\uparrow)$	97.45	18.64

[a] Arrows indicate spin directions in monomer units.

The L−H gaps between the LUMO's (↓) and HOMO's (↓) are about 2−3 eV smaller than the neutral ones. This is because the LUMO's (↓) and HOMO's (↓) in the triplet dications have the character of the second HOMO's and the third HOMO's in the neutral dimers. In the case of Y = O, the L−H gaps are the largest in all the dimers. Only in the case of **I** with Y = O are the L−H gaps of the triplet dications larger than those of the doublet monocations. In all the other systems, they are smaller.

5. Trimers and Tetramers

5.1 Energy Gaps between Different Spin States. The energy gaps between different spin states in *N*-mers, *N* = di, tri, and tetra, of type **II** trans connections for X = S and Y = CH_2 are listed in Table 6.

↑(↓) indicates the TFF on which a hole with ↑(↓) spin is present. The less the number of ↑−↓ pairs in spin configuration is, the lower the energy. Therefore, the trications of trimers and the tetracations of tetramers have quartet and quintet ground states, respectively. In the Ohno case, spin states exist at nearly regular energy intervals (about 6 eV). In tetramers, spin states with the same numbers of parallel and antiparallel spins lie close together with energy intervals about 0.1 eV. The energy gap between the ground and lowest excited states increases a little with increasing molecular length. In the M−N case, such closely lying levels and regular intervals are not present.

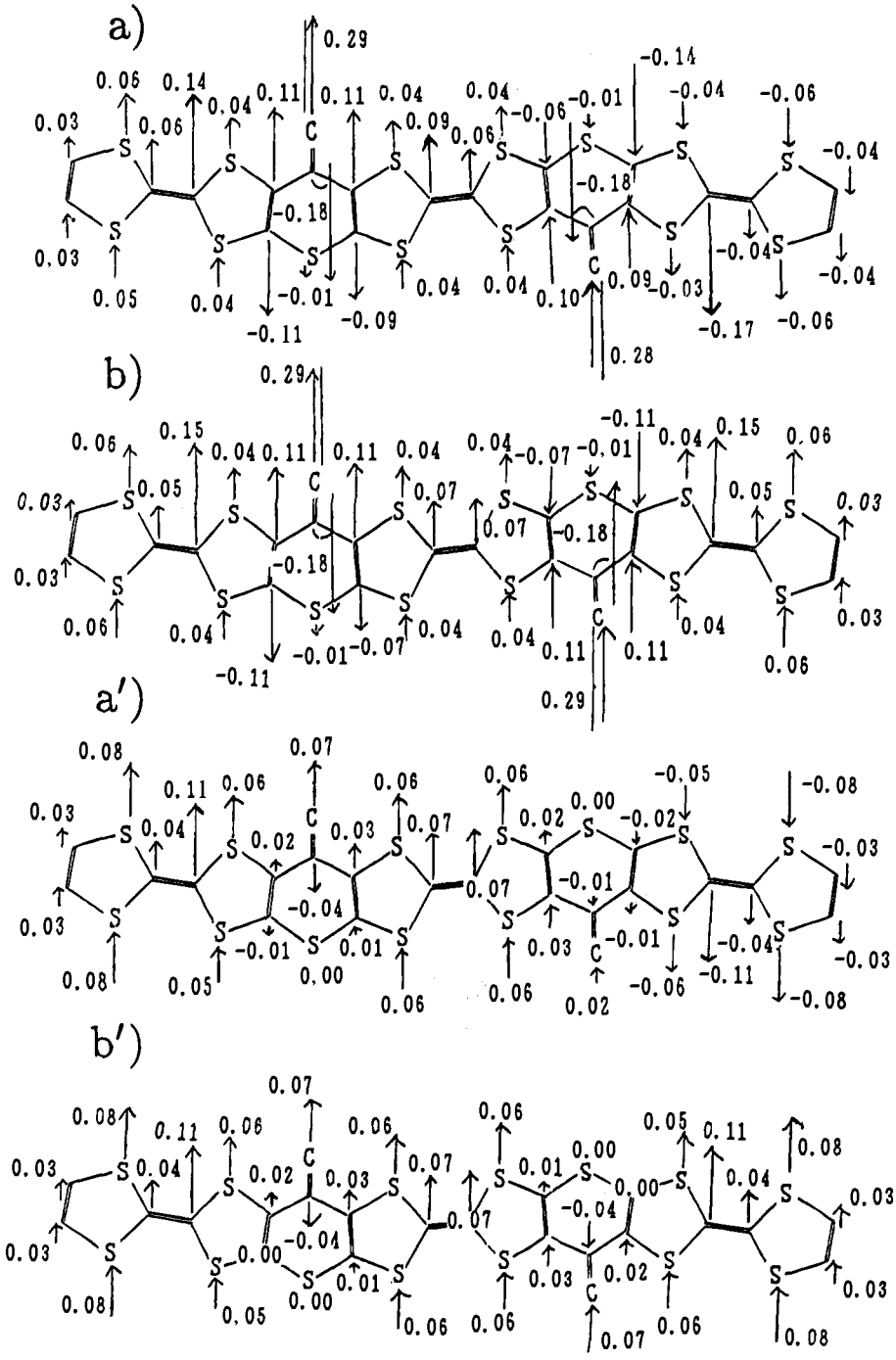

Figure 6. Spin density (SD) structures of trimers of **II** with X = S and Y = CH_2. a and b show the $S = {}^1/_2$ state with monomer spin arrangement (↑↑↓) and the $S = {}^3/_2$ state with monomer spins (↑↑↑), respectively, in the M−N potential case. a′ and b′ show corresponding states in the Ohno potential case.

Especially the energy gap between the ground and lowest spin excited states in *N*-mers is larger than the Ohno case and decreases much as *N* increases. Therefore, interactions of spins are dependent on *N*. These results show that oligomers will have high-spin ground states upon electron transfer of every momomer unit.

5.2 π Electron Density and Spin Density of Trimers and Tetramers. In trimers and tetramers, the spin delocalization on donors and the CP and DSP on the linking bonds appear as in dimers (Figure 2). But in the Ohno case, the DSP on the linking bonds is weak in ↑−↓ pairs.

The longer molecules have larger DSPs in ↑−↑ pairs, and this will be the origin of the small increase with *N* in the energy intervals (Table 6). Because the DSP in the Ohno case appears only on the linking bonds, unlike the M−N case, where the DSP is extended to a part of donors, stabilization due to the DSP can be roughly considered as the sum of the contributions from ↑−↑ and ↑−↓ pairs. This will be why spin excited states are present with nearly regular energy intervals. On the other hand, in the M−N case, the amount of the DSPs in trimers and tetramers is almost the same as in dimers, but the magnitudes of the DSPs are so large that they have substantial interactions much larger than the Ohno case. This may be the reason why the lowest energy gaps become narrower as the molecules become longer (Table 6).

6. Conclusions and Discussion

The above results are summarized as follows.

(1) The dications of the dimers of **I**, **II**, and **III** have the triplet ground states in the PPP−UHF calculations.

(2) The S−T gaps of the planar dimers of **II** are much larger than those of the nonplanar dimers of **I**. The dimers of **III** have the smallest S−T gaps.

(3) The triplet state is stabilized by the DSP in the connecting bonds. The DSP is small in the Ohno potential, giving small S−T gaps. It is large in the M−N potential, giving large S−T gaps. The DSP in **III** is small, about one-half of those in **I**, and gives very small S−T gaps.

(4) The tri- and tetracations of trimers and tetramers, respectively, connected similarly to **I** and **II** have the quartet and quintet ground states which are stabilized by the DSPs in the connecting groups.

(5) In the Ohno case, the energy intervals between different spin states have a regular pattern, owing to the small interaction between the small DSPs on different connecting groups. In the M−N case, the DSPs are large so that those on different connecting groups have large interactions. Consequently, there is no regular pattern in the energy intervals such as is observed in the Ohno case, but those between the ground and the lowest excited spin states decrease with increasing N.

(6) The HOMO's of the neutral of **I** and **II** are symmetrical or antisymmetrical combinations of the HOMO's of the neutral monomers, but their LUMO's have MO coefficients concentrated on the connecting group and have no relation to the LUMO of the monomer. Consequently, the L−H gaps of the neutral dimers are smaller than that of the monomer.

(7) In the triplet states of the dications of the dimers of **I** and **II**, where two down spin electrons are removed, the up spin LUMO's and HOMO's have characters similar to those in the neutral dimers, but the down spin LUMO's are the antisymmetrical combinations of the HOMO's of the monomers, and the HOMO's have concentrated weights on the connecting group contributing to the DSP on it. The L−H gaps in the dicationic triplet dimers are much smaller than those in the neutral dimers.

These donor oligomers may give high-spin ground states upon ET as the present PPP−UHF calculations have demonstrated. However, the calculated S−T gaps in the dimers are small, especially in the Ohno potential case. There may be several factors to reverse the order of the singlet and triplet states. In twisted dimers of **I**, interference between π and σ electrons may alter the order of these states. However, the inappropriateness of the full valence electron CNDO- and INDO-type models for TTF prevents confirmation of this possibility by explicit calculations.

Configuration interactions (CIs) may also reverse the order of the singlet and triplet states. We show in Table 7 the π EDs on the atom Y and the central carbon C_1 on the connecting bond in the dicationic dimers **I** and **II** with X = S. This shows that a large ET from C_1 to Y occurs when Y = O. About a one-half smaller ET occurs when Y = S, but little ET is taking place when Y = CH_2 and $C(CN)_2$. The large electron deficiency in C_1 by the ET yields intramolecular ET from TTFs to C_1 to neutralize C_1. Since an up spin electron is more deficient at C_1 in the M−N case (Figure 3), the intramolecular ET mainly transfers it to C_1, decreasing the DSP in the connecting bond, namely, stabilizing the singlet state. In the Ohno case, the DSP is very small in spite of the large ET from C_1 to O (Figure 3).

Table 7. π EDs on the Atom Y and the Central Carbon C_1 on the Connecting Bonds in the Dicationic Dimers **I** and **II** with X = S[a]

		I		II	
X	Y[f]	M−N	Ohno	M−N	Ohno
S	CH_2	0.97	0.93	0.99	0.97
	C_1	1.02	1.05	1.02	1.04
	O	1.35[b]	1.44	1.40[c]	1.48
	C_1	0.75[d]	0.64	0.77[e]	0.65
	S	1.16	1.23	1.20[b]	1.30
	C_1	0.90	0.82	0.91[d]	0.82
	$\underline{C}(CN)_2$	0.99	1.01	1.01[b]	1.07
	$\underline{C}_1$	0.99	0.99[e]	0.99	0.95
	$C(\underline{C}N)_2$	0.86	0.83	0.86	0.81
	$C(\underline{C}N)_2$	1.16	1.19	1.17	1.22

[a] EDs in the triplet and singlet states are the same in most cases. The values in the triplet state are shown. [b] The EDs in the singlet state are larger by 0.01. [c] The EDs in the singlet state are larger by 0.03. [d] The EDs in the singlet state are smaller by 0.01. [e] The EDs in the singlet state are smaller by 0.02. [f] For Y = $C(CN)_2$, the atom, for which its ED is shown, is indicated by the underline.

Recently, Sugimoto et al.[28] synthesized the dimers with X = S and Y = O without and with a substituent at C_3, CO_2CH_3, or $CON(CH_3)_2$. All the dicationic dimers in solution showed doublet ESR signals, showing that there was no interaction between two TTFs. Unsubstituted dicationic dimers were cooled to −268 °C. They gave a doublet ESR signal markedly weaker than in solution. It was concluded that the ground state of the dicationic dimers that is not twisted so much is the singlet state. This example shows the importance of CIs in the present systems. However, Table 7 shows that there are little ETs between C_1 and Y in the cases of Y = CH_2 and $C(CN)_2$, so that these systems may have the triplet ground state. The case Y = S may be intermediate between these two extreme cases. Therefore, we need further studies to confirm the theoretical predictions in this paper. Since reliable theoretical CI studies are difficult to perform, it will be better to try to synthesize Y = CH_2 dimers especially of type **II**.

Acknowledgment. The work was supported in part by a grant from the International Joint Research Project from the NEDO, Japan, and in part by a Grant-in Aid for Scientific Research on Priority Area "Molecular Magnetism" (Area No. 228/04242101) from the Ministry of Education, Science, and Culture, Japan. Numerical computation in this work was supported in part by the Yukawa Institute for Theoretical Physics.

JA943483D

(28) Sugimoto, T.; Yamaga, S.; Nakai, M.; Nakatsuji, H.; Yamauchi, J.; Fujita, H.; Fukutome, H.; Ikawa, A.; Mizouchi, H.; Kai, Y.; Kanehisa, N. *Adv. Mater.* **1993**, *5*, 741−743.